Evidence for Precursors of the Coronal Hole Jets in Solar Bright Points

S.R. Bagashvili[1,3,4], B.M. Shergelashvili[2,1,4], D.R. Japaridze[1], V. Kukhianidze[1], S. Poedts[3], T.V. Zaqarashvili[2,1,5], M. L. Khodachenko[2], P. De Causmaecker[4]

1 **Abastumani Astrophysical Observatory at Ilia State University, Giorgi Tsereteli 3, Tbilisi, Georgia**
2 Space Research Institute, Austrian Academy of Sciences, Schmiedlstrasse 6, 8042 Graz, Austria
3 Center for Mathematical Plasma Astrophysics, Department of Mathematics, KU Leuven, 200 B, B-3001, Leuven, Belgium
4 Combinatorial Optimization and Decision Support, KU Leuven campus Kortrijk, E. Sabbelaan 53, 8500 Kortrijk, Belgium
5 Institute of Physics, IGAM, University of Graz, Universitatsplatz 5, 8010 Graz, Austria

Abstract: A set of 23 observations of coronal jet events that occurred in coronal bright points has been analyzed. The focus was on the temporal evolution of the mean brightness before and during coronal jet events. In the absolute majority of the cases either single or recurrent coronal jets (CJs) were preceded by slight precursor disturbances observed in the mean intensity curves. The key conclusion is that we were able to detect quasi-periodical oscillations with characteristic periods from sub-minute up to 3–4 minute values in the bright point brightness that precedes the jets. Our basic claim is that along with the conventionally accepted scenario of bright-point evolution through new magnetic flux emergence and its reconnection with the initial structure of the bright point and the coronal hole, certain magnetohydrodynamic (MHD) oscillatory and wavelike motions can be excited and these can take an important place in the observed dynamics. These quasi-oscillatory phenomena might play the role of links between different epochs of the coronal jet ignition and evolution. They can be an indication of the MHD wave excitation processes due to the system entropy variations, density variations, or shear flows. It is very likely a sharp outflow velocity transverse gradients at the edges between the open and closed field line regions. We suppose that magnetic reconnections can be the source of MHD waves due to impulsive generation or rapid temperature variations, and shear flow driven nonmodel MHD wave evolution (self-heating and/or overreflection mechanisms).

Observations and Methodology of Data Analysis

We used data from the Atmospheric Imaging Assembly (AIA) on board of the Solar Dynamic Observatory (SDO). The SDO/AIA data are retrieved, processed, and analyzed using standard procedures with the SolarSoft package.

We have studied BPs and CJs situated within and at the edges of the CHs. The CHs have been chosen from different areas of both hemispheres, during the period from 2015 December 1 until 2016 May 1. In total, we investigated 23 CJs using SDO/AIA 193 Å channel images.

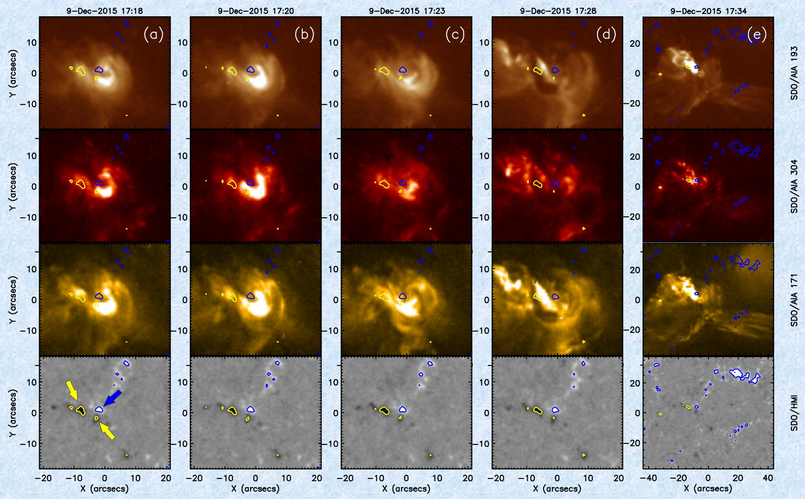

Figure 1. Sample BP before and during CJ ejection process. The top three rows represent overlap of SDO/AIA 193, 304, and 171 Å intensity images and SDO/HMI photospheric magnetograms. The bottom row represents HMI magnetogram separately. Blue and yellow contours indicate positive and negative magnetic field polarities, respectively. These regions are also indicated with arrows in the bottom row of panel (a). Panel (a): the beginning of precursor; panel (b): the peak of the precursor brightening; panel (c): the time after the precursor when still there is no signature of main jet outflow; panel (d): the moment when the structure is destabilized and the jet-type instability starts; panel (e): the fully developed transient jet outflow. In panel (e), we take a wider observational window as shown on the corresponding axes.

We created two types of 193 Å intensity curves (Figure 2). The first type of data (data set 1) comprises the calculation of the mean intensity values of the entire cutout BP-boxes. The second type of data (data set 2) is created using the average over all pixels of modified intensity value cutout BP-boxes obtained through noise deduction. Consequently, in data set 2, the effect of background noise is removed and all the transient disturbances are more sharply observable. Examples of brightness evolution curves are shown in the top panels (CJ1) and (CJ2/CJ3/CJ4) of Figure 2.

Analysis of the Results

This study uncovers the systematic presence of relatively low amplitude (compared to the jets) quasi-oscillatory dynamic processes before each main jet event (the solid-line, black parts of the curves in the top panels (CJ1) and (CJ2/CJ3/CJ4) of Figure 2). We argue that these processes can represent precursors of jets (the solid-line, red and blue colored parts of the curves in the top panels (CJ1) and (CJ2/CJ3/CJ4) of Figure 2).

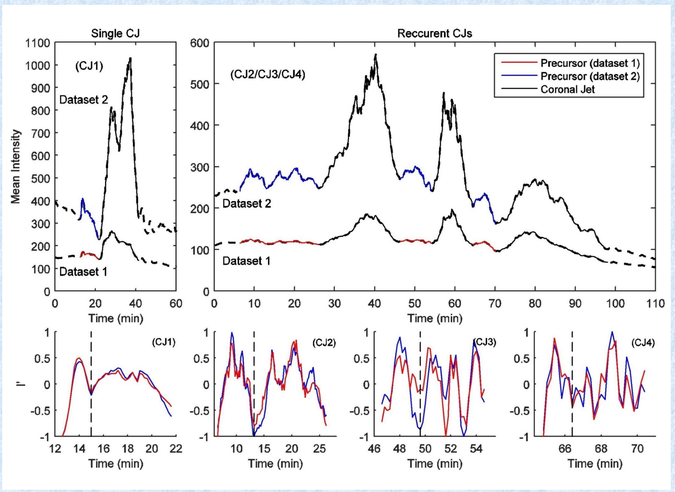

Figure 2. Coronal jet intensity curves for data set 1 (without threshold—bottom curves) and data set 2 (with threshold—top curves) in the top panels (CJ1) and (CJ2/ CJ3/CJ4). Red (data set 1) and blue (data set 2) solid-line parts of the curves indicate precursors events. Accordingly, we plot zooms of these parts in the detrended form in the bottom panels (CJ1), (CJ2), (CJ3), and (CJ4), respectively. Panels (CJ1; top and bottom) correspond to the case of the single CJ that started at 2015 December 9 17:28 UT with a precursor start approximately 9.8 minutes before the CJ release. While panels (CJ2/CJ3/CJ4), (CJ2), (CJ3), and (CJ4) demonstrate the case of the recurrent CJs that started at 2015 December 30 23:16 UT, which includes three subsequent plasma ejections. Each of them has precursors starting 19.6, 7.8, and 5.6 minutes before the respective CJs. Vertical dashed lines represent the end of precursor ignition.

Further, we plot these precursor parts zoomed in and detrended for an isolated single (top panel (CJ1)) and for a recurrent jet event (panels (CJ2), (CJ3), and (CJ4)). The corresponding FFT periodograms are presented in Figure 3.

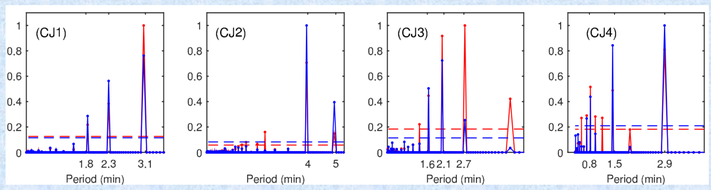

Figure 3. Set of calculated FFT periodograms accordingly corresponding to cases shown in the bottom panels (CJ1), (CJ2), (CJ3), and (CJ4) of Figure 2. The coloring is the same as in Figure 2, and horizontal blue and red dashed lines represent 95% confidence levels for data set 2 and data set 1, respectively. The spectral powers are normalized on the maximum power pick shown in each panel.

In the absolute majority of instances (20 out of 23) we detect a characteristic brightening of the observed BP preceding, by a few minutes, the main jet outflows. We consider these processes as CJ precursors (as shown in Figure 2).

The enhancement of the BP intensity is visible several minutes before the CJ ejection in the case of both data set 1/data set 2 mean intensity curves. In both cases of single and recurrent jets, the precursors are systematically observed before each plasma ejection. In the top panel (CJ1) of Figure 2, the existence of the precursor of the single jet event is evident (2015 December 9 17:18 UT). Besides, the set of recurrent events in panel (CJ2/CJ3/CJ4) of Figure 2 took place within the time interval from 2015 December 30 23:01 UT to 2015 December 31 00:31 UT and included three consecutive plasma ejections, each of them had corresponding precursors.

Finally, for the 23 investigated events a precursor was found in 20 cases. The detailed catalog of the investigated CJ parameters is presented in Table 1.

We investigated the statistical distributions of the precursor and the CJ individual parameters. These parameters with related variance and error estimations are presented in Table 2 .

Parameters of CJs and Their Precursors

No.	Obs. Start Time	Location	Type	τ_{PI}	τ_{PT}	τ_{CJ}	$\Delta\tau_{Peaks}$	Osc. Periods
CJ1	2015 Dec 09 17:18	355, −260	S	1.75/1.28	9.4/9.8	7.16/8.13	13.55/14.49	1.8–3.1
CJ2	2015 Dec 30 22:56	−780, −270	R	4.58/4.78	19.6/19.6	9.20/10.15	13.83/13.31	4.0–5.0
CJ3	2015 Dec 30 23:40	−780, −270	R	2.78/2.27	7.8/7.8	4.85/5.54	8.03/8.02	1.6–2.7
CJ4	2015 Dec 30 23:58	−780, −270	R	2.59/1.51	5.6 /5.6	16.38/16.96	13.11/12.59	0.7–2.9
CJ5	2015 Dec 31 02:12	−770, −280	R	4.40/3.86	13.6/13	11.77/11.33	20.78/20.95	1.4–4.6
CJ6	2015 Dec 31 02:52	−770, −280	R	2.97/3.05	8/8	6.23/5.96	14.27/14.14	0.9–3.4
CJ7	2015 Dec 07 15:56	385, 510	R	13.82/12.72	21.2/20	13.49/15.60	20.64/23.80	1.9–5.1
CJ8	2015 Dec 07 17:08	385, 510	R	3.17/3.85	4.9/5.4	8.05/8.24	9.49/8.96	1.2–2.1
CJ9	2015 Dec 08 11:38	15, −225	S	4.73/5.03	20 /20.2	6.38/4.42	19.92/19.43	2.3–4.1
CJ10	2015 Dec 05 09:11	430, 230	S	1.72/1.62	2.2/2.2	9.21/8.43	5.71/6.50	0.5–1.2
CJ11	2015 Dec 10 19:25	765, −230	R	5.79/6.09	14.6/13.8	5.64/6.50	15.39/15.57	1.2–3.7
CJ12	2015 Dec 10 21:04	765, −235	R	5.90/5.91	7.8/7.8	10.77/10.52	11.05/11.58	1.0–4.0
CJ13	2016 Mar 21 21:30	515, 585	S	12.02/12.59	12.59/12.59	12.02/12.59	0/0	…
CJ14	2016 Mar 21 21:21	630, 435	S	6.73/6.49	11.6/10.4	11.80/11.51	11.45/12.46	0.8–1.9
CJ15	2016 Mar 22 02:40	−705, −130	R	3.57/4.05	4.05/4.05	3.57/4.05	0/0	…
CJ16	2016 Mar 22 02:55	−660, −80	R	9.44/9.06	9.06/9.06	9.44/9.06	0/0	…
CJ17	2016 Apr 18 10:44	−460, 275	S	1.86/1.89	3.2/3.2	3.36/3.32	3.24/3.15	0.4–1.7
CJ18	2016 Apr 18 13:39	−550, 445	S	2.70/2.22	4.4/3.4	10.40/9.96	8.99/10.37	0.9–1.5
CJ19	2016 Apr 18 14:08	−520, 385	S	0.93/0.88	2/2.2	6.28/5.42	9.12/8.81	0.8–1.2
CJ20	2016 Apr 18 16:58	605, 460	R	3.77/3.34	4/6.0	9.87/10.35	17.59/17.05	0.5–2.1
CJ21	2016 Apr 18 21:25	640, 450	R	1.81/2.36	3.2/3.2	6.35/5.99	6.40/6.15	0.5–1.1
CJ22	2016 Apr 18 21:57	640, 450	R	1.90/1.90	2.4/2.4	6.39/5.81	5.28/5.34	0.5–0.6
CJ23	2016 Apr 18 18:25	−485, 385	S	3.03/3.08	6.2/6.6	6.12/4.91	8.54/8.27	1.8–3.6

Table 1. Sample Complete set of 23 selected CJ and corresponding precursor parameters. Location represents BP (x, y) coordinates in arcsecs; in the column Type we have two possible values S—single and R—recurrent; τ_{PI} represents the precursor ignition duration; τ_{PT} is the precursor total evolution time span; (τ_{CJ})—CJ durations, $\Delta\tau_{Peaks}$ —the time intervals between precursor and CJ peaks; Osc. Periods shows the minimum and maximum values of precursor oscillation periods. The parameters having time dimension are measured in minutes.

Parameters Average Values CJs and Their Precursors

Parameters x	Maximum Probability f_0	Expected Value $\bar{x}$	σ (Variance)	Error $= \sigma/\sqrt{N}$
τ_{PI}	0.21/0.22	2.77/2.85	1.35/1.29	±0.28/±0.27
τ_{PT}	0.13/0.15	5.95/5.92	4.26/4.09	±0.89/±0.85
$\Delta\tau_{Peaks}$	0.12/0.11	10.25/10.13	6.83/7.59	±1.43/±1.58
τ_{CJ}	0.18/0.18	8.52/8.62	4.03/4.28	±0.84/±0.89
I_{CJ}/I_{PI}	0.31/0.28	2.18/2.59	0.80/1.12	±0.17/±0.23
τ_{CJ}/τ_{PI}	0.17/0.19	2.02/1.69	1.16/0.95	±0.24/±0.20
$\Delta\tau_{Peaks}/\tau_{PI}$	0.23/0.20	2.72/2.56	1.38/1.69	±0.29/±0.35
$\Delta\tau_{Peaks}/\tau_{CJ}$	0.16/0.16	1.36/1.34	0.67/0.67	±0.14/±0.14
Min. osc. period	…	1.24	0.83	±0.18
Max. osc. period	…	2.77	1.34	±0.30

Table 2. The CJ and corresponding precursor parameters with related variance and error estimations. τ_{PI} represents the precursor ignition duration; τ_{PT} is the precursor total evolution time span; (τ_{CJ})—CJ durations, $\Delta\tau_{Peaks}$—the time intervals between precursor and CJ peaks. All the quantities in the top four rows are measured in minutes and in the bottom four rows all are dimensionless. All values are given in accordance with the order data set 1/data set 2. In the two bottom rows, values are calculated in minutes and only for data set 2.

Discussion and Conclusions

The key conclusion that can be drawn from our analysis is that we were able to detect quasi-periodical oscillations with characteristic periods from sub-minute up to 3–4 minute values in the BP brightness that precede the jets. The basic claim that can be made at this stage of pure observational analysis is that along with the conventionally accepted scenario of BP evolution through new magnetic flux emergence and its reconnection with the initial structure of the BP and the CH, certain MHD oscillatory and wavelike motions can be excited and these can take an important place in the observed dynamics. One can even imagine that these quasi-oscillatory phenomena might play the role of links between different epochs of the CJ ignition and evolution. A complete understanding of this issues requires further analytical and perhaps even numerical modeling of the processes, and such investigations will become a matter of future more extensive studies. However, we can make some general qualitative indications on the observed oscillatory processes and their link with some theoretical background. The quasioscillatory variations of intensity can be an indication of the MHD wave excitation processes due to the system entropy variations (Shergelashvili et al. 2007) or density variations (Zaqarashvili & Roberts 2002; Shergelashvili et al. 2005). The observed mutual positioning of open and closed magnetic field structures indicates that there is very likely a sharp outflow velocity gradients at the edges between the open and closed field line regions. All these conditions suggest a sequence of local magnetic reconnection events that could be the source of MHD waves due to impulsive generation or rapid temperature variations (Shergelashvili et al. 2007), on the one hand, and shear flow driven MHD wave excitation, coupling, and dissipation (self-heating mechanism) processes (Shergelashvili et al. 2006) and explosive type strongly non-adiabatic overreflections in the shear flows (Gogoberidze et al. 2004), on the other hand.

References:

Gogoberidze, G., Chagelishvili, G. D., Sagdeev, R. Z., & Lominadze, D. G. 2004, PhPl, 11, 4672
Shergelashvili, B. M., Maes, C., Poedts, S., & Zaqarashvili, T. V. 2007, PhRvE, 76, 046404
Shergelashvili, B. M., Poedts, S., & Pataraya, A. D. 2006, ApJL, 642, L73
Shergelashvili, B. M., Zaqarashvili, T. V., Poedts, S., & Roberts, B. 2005, A&A, 429, 767
Zaqarashvili, T. V., & Roberts, B. 2002, PhRvE, 66, 026401